Is the Stillinger and Weber decomposition relevant for coarsening models?

2002 J. Phys.: Condens. Matter 14 1523

(http://iopscience.iop.org/0953-8984/14/7/310)

INSTITUTE OF PHYSICS PUBLISHING JOURNAL OF PHYSICS: CONDENSED MATTER

J. Phys.: Condens. Matter **14** (2002) 1523–1538 PII: S0953-8984(02)31984-2

Is the Stillinger and Weber decomposition relevant for coarsening models?

A Crisanti[1,2], F Ritort[3], A Rocco[1,2,4] and M Sellitto[5]

[1] Dipartimento di Fisica, Università di Roma 'La Sapienza', Piazzale Aldo Moro 2, I-00185 Roma, Italy
[2] Istituto Nazionale Fisica della Materia, Unità di Roma, Italy
[3] Departament FFN, Facultat de Física, Universitat de Barcelona, Avenida Diagonal 647, 08028 Barcelona, Spain
[4] CWI, Postbus 94079, 1090 GB Amsterdam, The Netherlands
[5] Abdus Salam International Centre for Theoretical Physics, 34100 Trieste, Italy

Received 18 December 2001
Published 7 February 2002
Online at stacks.iop.org/JPhysCM/14/1523

Abstract

We study three kinetic models with constraint, namely the symmetrically constrained Ising chain, the asymmetrically constrained Ising chain, and the backgammon model. All these models show glassy behaviour and coarsening. We apply to them the Stillinger and Weber (SW) decomposition, and find that they share the same configurational entropy, despite their different non-equilibrium dynamics. We conclude therefore that the SW decomposition is not relevant for models of this type.

1. Introduction

The description of glassy dynamics remains an intriguing issue, even after years of research [1]. In this context considerable progress has been achieved by the introduction of *constrained kinetic Ising models*. In these models the *slowing down* of the dynamics is realized through the introduction of microscopic kinetic constraints, which serve the purpose of preventing certain spins from being flipped. The first proposal was made by Fredrickson and Andersen in 1984 [2] in the attempt to provide a simple microscopic mechanism for understanding the purely dynamical transition predicted by the mode-coupling theory. Along the same lines, Jäckle and Eisinger [3] later on modified that model, inserting a stronger constraint which results in an exponential inverse temperature squared dependence for the relaxation time [4]. More recently, constrained Ising chains have also been considered as simple models for granular compaction [5]. As a matter of fact, all these models show *glassy behaviour* in the sense that their relaxation times diverge when temperature is lowered [6]. Their relaxation toward equilibrium proceeds through the coalescence of domains of either up or down spins. This process is characterized by a *growing length scale* (the average domain length), which drives the system toward equilibrium and signals the *coarsening behaviour* of these models.

As is well known, the description of the slow dynamics of either spin glasses or structural glasses rests on the idea of the exploration of the configuration space through thermal jumps (*activated dynamics*). The more the temperature is lowered, the more the system gets confined in localized regions of the phase space, pretty much as a golf ball gets trapped in the valleys of the green. Whether or not coarsening can be considered as another prototype process relevant to the description of the glassy dynamics is an open question. Probably a reasonable answer calls for the superposition of the two processes, namely coarsening and activation.

In the case of systems exhibiting mainly activated dynamics, an interesting approach was proposed by Stillinger and Weber (SW) in the early 1980s [7]. Their approach was based on the decomposition of the configuration space into *valleys* on the basis of the topology of the potential energy landscape. To each valley a label, called the inherent structure (IS), is attached, and the off-equilibrium dynamics of the system is reduced to a dynamics defined on the IS configurations. This projection technique has been proven to be relevant to the glass transition in several cases, in the domain of both potential [8, 9] and free energy [10].

An interesting question, however, is whether or not this approach can be straightforwardly applied to coarsening systems too. The question is far from trivial because for these systems, on top of the activated dynamics, there is also a geometrical constraint leading the system to explore the configuration space along a coarsening path. In contrast to what happens for purely activated dynamics, now, once the systems sits in some valley, the choice of the next one to reach via a thermally activated jump is not simply related to the number and dimensions of the neighbouring valleys, but is also driven by the constraint that the average domain length must grow with time. Therefore the suspicion that the SW decomposition may be not able to reproduce the off-equilibrium behaviour of these systems is legitimate and requires specific attention. As we shall see, it seems that indeed the SW decomposition does not capture the specific dynamics of coarsening models.

The paper is organized as follows. In the next section we shall present the models under study, namely the symmetrically and the asymmetrically constrained Ising chain. The backgammon model (BG) will also be introduced for comparison. Then, in section 3 we shall analyse the response of these models to perturbations, discussing their fluctuation-dissipation relations. In section 4 we shall present the SW decomposition and show that the corresponding configurational entropy does not account for the different dynamics of these systems. Finally in section 5 we shall draw some conclusions.

2. The models

2.1. The symmetrically constrained Ising chain (SCIC)

The SCIC was first introduced by Fredrickson and Andersen [2] in 1984. The model is defined as follows:

$$E = -\sum_{i=1}^{N} \sigma_i \tag{1a}$$

$$\mathcal{W}(\sigma_i \to 1 - \sigma_i) = \tfrac{1}{2}[2 - \sigma_{i-1} - \sigma_{i+1}] \min\{1, \mathrm{e}^{-\beta \Delta E}\}. \tag{1b}$$

Here the variables σ are Ising-like spin variables, which can take the values 0 (down spin) or 1 (up spin). The ordinary Glauber rule is defined on a restricted class of mobile spins, thereby making the dynamics of the model far from being trivial. More specifically, the constraint present in the transition probability makes the ordinary update possible only for those spins whose left or right first neighbour is found in the down state. For all the other spins the corresponding transition rate is zero. As a result, even though the energy of the system

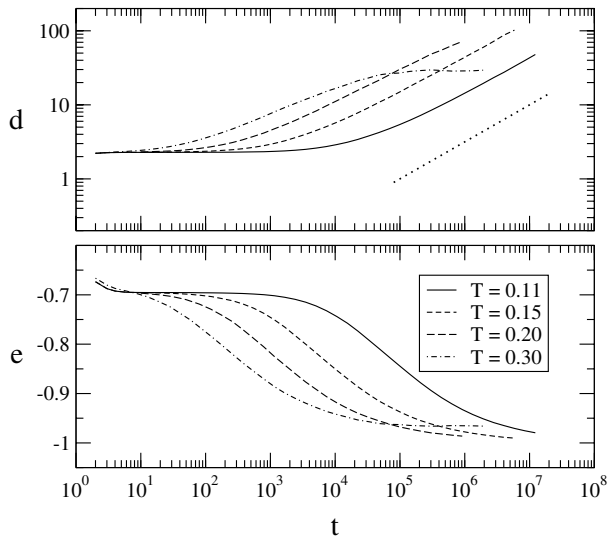

Figure 1. Relaxation of average domain length and energy in the SCIC at different temperatures. The dotted line corresponds to the power law $t^{1/2}$.

simply corresponds to a paramagnet in a field, its dynamics turns out to be much richer, and in particular the approach toward equilibrium is expected to show slow motion properties.

To get more insights into the relaxation properties of the model, let us discuss briefly its microscopic dynamics, as defined by (1). Starting from an initial condition where each spin is assigned randomly the value 0 or 1, there will be an initial situation, characterized by a timescale which will be specified in the following, where a quite fast growth of small *domains* of spins in the up state will occur. These domains will be separated by spins in the down state, which from now on will be called *defects*. After this initial phase, the equilibration of the system will proceed through the process of eliminating defects. This is where the constraint enters strongly into play. By definition of a defect, both its neighbours are in the up state, and therefore its flipping is forbidden. The only possibility of eliminating it will be to carry another defect (*auxiliary defect*) to its right or left, forcing it to travel along one of the two adjacent domains. This process is clearly slow because the travelling of the auxiliary defect toward the original one will involve the overturning of up spins into down spins, with an increase of the energy of the system as determined by the Metropolis factor. Then it will become possible to flip the original defect, and, when flipped, one of the two adjacent domains will increase its length by one unit. To complete the process, we still need to make the auxiliary defect travel back to its original position. Once this situation is achieved, the two original domains will have coalesced into a single one, with no other change in the chain of spins, and the energy will indeed have decreased. This is what we mean by *coarsening*. Note that this process will be slower and slower the closer the system is to equilibrium, since the domains of up spins get longer and longer with time. This is the origin of the glassy behaviour of the model. The relaxation of both average domain length and energy is shown in figure 1 for different temperatures. It is easy to show that regardless the dynamical rules the two quantities are related via $d = -e/(1 + e)$ [11], so the use of d or e is just a matter of taste.

The dynamics of the model is characterized by the existence of three relevant timescales. The first timescale has an Arrhenius behaviour and is strongly dependent on the constrained dynamics. It corresponds to the microscopic relaxation of one spin with its nearest neighbours

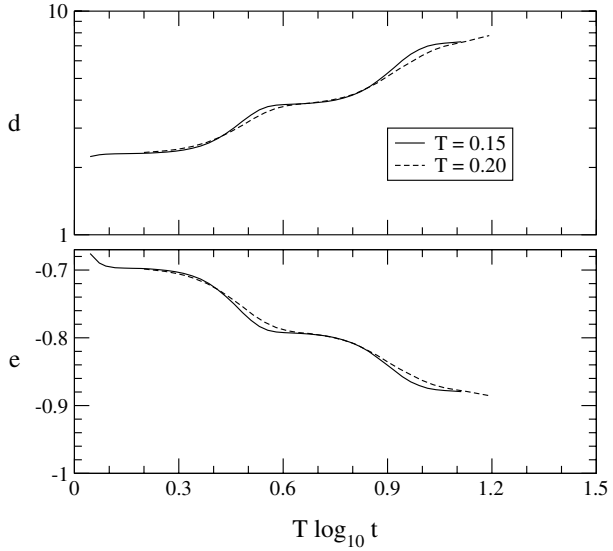

Figure 2. Relaxation of average domain length and energy in the ACIC model at $T = 0.15$ and 0.20.

(local equilibration) and can be evaluated to be $\tau_1 \sim \exp(\beta)$ [12]. Only for times larger than τ_1 will non-equilibrium behaviour appear, with non-exponential relaxation and aging effects. Another relevant timescale is the equilibration time which can be estimated as $\tau_{\rm eq} \sim \exp(\lambda\beta)$ with λ in the range 3–4. In fact a simple scaling analysis shows that $\lambda \sim 3$ [6]. Finally one can also define a correlation time $\tau_{\rm corr} \sim \exp(2\beta)$ as the integral of the equilibrium-connected correlation function [6]. This dependence on temperature is in agreement with the previous results of [13,14]. Note in figure 1 the initial plateau related to the timescale τ_1 and the diffusive growth of the average domain length.

2.2. The asymmetrically constrained Ising chain (ACIC)

The ACIC [3] is defined in a similar way to the SCIC:

$$E = -\sum_{i=1}^{N} \sigma_i \tag{2a}$$

$$\mathcal{W}(\sigma_i \to 1 - \sigma_i) = [1 - \sigma_{i-1}] \min\{1, \mathrm{e}^{-\beta \Delta E}\}. \tag{2b}$$

The basic difference is in the type of constraint used. In this case, the class of mobile spins is identified as those for which the left neighbour is in the down state. This makes the model more constrained than the SCIC, slowing the relaxation dynamics down even more. In particular, while in the SCIC a given defect can be reached by an auxiliary defect from either the left or the right domain, in the ACIC this can be done only from the left, due to the asymmetric nature of the constraint. This is well illustrated by the relaxation of both energy and average domain length, as shown in figure 2. The plateaus present during the relaxation process are a mark of the asymmetry of the constraint. They are not present in the SCIC model because in that case the system has the freedom to choose the fastest way of coalescing domains, meaning that the auxiliary defect will naturally travel through the shortest of the two domains adjacent to the defect to be eliminated. This produces in the SCIC a slow but continuous relaxation

of both energy and average domain length. In contrast, the ACIC model does not possess the same freedom, and domains can grow only leftwards, no matter whether this is the fastest way of achieving coalescence or not. As a result, both energy and average domain length display characteristic plateaus corresponding to the time needed for the flipping of up spins into down spins, related to the time it takes an auxiliary defect to travel across larger and larger domains. During this time the system is almost frozen. Of course this effect becomes more and more noticeable as the temperature becomes lower and results in the typical staircase shape for $T = 0$ [4].

The different nature of the constraint is also apparent in the timescales of the system. In this case only one timescale is present. It has been evaluated as $\tau \sim \exp(\beta^2/\lambda)$ with $\lambda = \log 2$ in [4, 15], and has been shown to correspond to both correlation and equilibration time [4]. Note the inverse square temperature dependence in the activated barrier, in contrast to the SCIC model case.

2.3. The backgammon (BG) model

Let us finally address the last model analysed in this paper, that is the BG model. The model was introduced by one of us [16] in 1995. It is defined as

$$E = -\sum_{i=1}^{N} \delta_{n_i,0} \tag{3a}$$

$$\mathcal{W} = \min\{1, \mathrm{e}^{-\beta \Delta E}\} \tag{3b}$$

where $n_i = 0, 1, \ldots, N$ is the occupation number of each site of a D-dimensional lattice of $N = L^D$ sites (in the following $D = 1$). The model can be pictured as an ensemble of N particles occupying N boxes, with the energy of the system given by the number of empty boxes. Even though this is not strictly speaking a kinetically constrained model, an effective constraint is still present in the form of the conservation of the total number of particles.

Particles can move from one box to another one with a probability given in terms of temperature by the ordinary Metropolis factor. Once the starting box is specified, different choices can be made on how to select the arrival box. In the original paper [16] both the starting and the arrival box were chosen randomly. The relaxation of the model, characterized by a mean-field dynamics which turned out to be exactly solvable [17], was then proven to rest on the overcoming of entropic barriers. In contrast we assume here a dynamics where particles can move only to nearest-neighbour boxes, introducing thereby activated processes as relevant processes in the relaxation properties of the system. This change is expected to introduce a coarsening behaviour, which was absent in the original model.

More specifically, after an initial fast evolution of the system, a situation will be achieved where multiply occupied boxes are separated by empty boxes and singly occupied boxes (*defects*). Then two types of microscopic process can take place. A first possibility is the wandering of a defect until it gets to a multiply occupied box. During this process no change in the energy of the system will occur, implying that the process is entropically driven. In fact, the decrease of the energy when the defect sticks to a multiply occupied box is related to the discovery of the right path in the configuration space to get to that multiply occupied box. This process is clearly entropic. On the other hand, the annihilation of two multiply occupied boxes also requires activation. In this case the creation of a defect is involved, and this is an activated process since an empty box must be occupied, leading thereby to an increase of the energy. As a result, this version of the model shows a coarsening behaviour related to the increase of the size of *domains of empty boxes*. In figure 3 we report the behaviour of energy and average

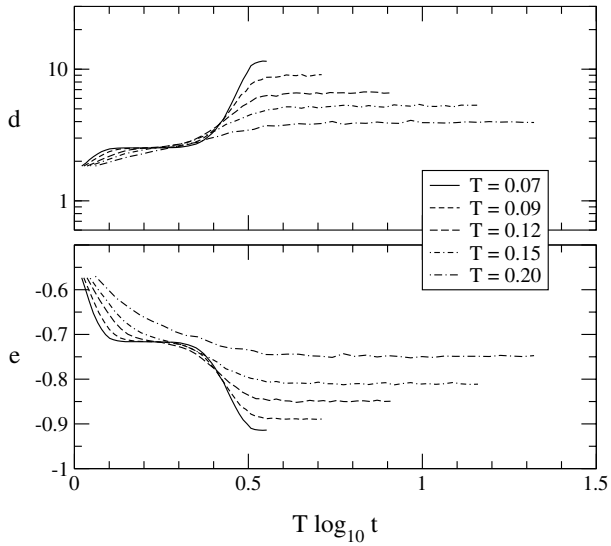

Figure 3. Average domain length and energy in the BG model. The plateau appearing at lower temperatures is related to the microscopic timescale τ_1 and is representative of the time spent by the system in the entropic elimination of defects.

domain length at different temperatures. It is easy to show that also for this model d and e are related via $d = -e/(1+e)$.

According to the presence of the two processes mentioned above, two timescales are present in the system. The first timescale is associated with the entropic mechanism and is estimated in [6] as $\tau_1 \sim \exp(\beta)/\beta$. This timescale plays a similar role as the timescale τ_1 defined in the SCIC model. The equilibration of the system, on the other hand, proceeds via the activated mechanism described above and is estimated again in [6] as $\tau_{\rm eq} \sim \beta \exp(\beta)$. The interplay between these two different timescales is shown in figure 3.

Finally let us remark that this model, too, clearly shows glassy dynamics since after the initial elimination of defects the successive elimination of multiply occupied boxes becomes slower and slower as time goes on, and this effect increases exponentially as the temperature is lowered.

3. Fluctuation-dissipation relation

In the previous section we have seen that the models under study are characterized by different dynamics. All of them are constructed in such a way as to exhibit both coarsening and glassy behaviour. Nevertheless the different natures of the constraints inserted results in the existence of different timescales, and produces different relaxation features.

In order to get more insights into the different dynamics of these models we analyse their response to an external perturbation. An efficient way of doing this is through the so-called fluctuation-dissipation plots [18], where the response is plotted as a function of the correlation.

First of all, we need to define a suitable perturbation. This must be chosen in such a way that the linear response regime applies and also it must be not coupled with the absorbing state,

that is the ground state. A good choice is the following:

$$\delta\mathcal{H}(t) = -h_0\Theta(t - t_w)\sum_{i=1}^{N}\epsilon_i\sigma_i. \tag{4}$$

Here h_0 is a (small) constant external field, and ϵ_i are just zero mean random quenched variables which can take the values ± 1. After an initial free evolution starting from a random configuration, the perturbation is turned on at time t_w. The spin variables are the usual ones defined in the SCIC and ACIC models and are defined as $\sigma_i = \delta_{n_i,0}$ in the BG model.

Accordingly we measure the correlation function,

$$C(t + t_w, t_w) = \frac{1}{N}\sum_{i=1}^{N}\nu_i(t_w)\nu_i(t + t_w) \tag{5}$$

and the staggered magnetization,

$$M_{\mathrm{stag}}(t + t_w, t_w) = \frac{1}{N}\sum_{i=1}^{N}\epsilon_i\nu_i(t + t_w). \tag{6}$$

For reasons that will become clear shortly, we used the variables $\nu_i = 2\sigma_i - 1$ in place of the σ_i.

In general, at equilibrium, for any two times t and t', correlation C and response R are related by the fluctuation-dissipation theorem (FDT) as

$$R(t - t') = \beta\frac{\partial C(t - t')}{\partial t'} \tag{7}$$

where the explicit dependence on the two times is lost due to the invariance under time translation at equilibrium. Defining the integrated response function as

$$\chi(t - t') = \int_{t'}^{t}\mathrm{d}u\, R(t, u). \tag{8}$$

Equation (7) can be rewritten as

$$\chi(t - t') = \beta[C(0) - C(t - t')] = \beta[1 - C(t - t')] \tag{9}$$

where the second equality holds when the variables ν_i are assumed. Then plotting $T\chi$ as a function of C will result in a straight line with slope -1.

Of course these properties are not expected to be valid if the regime under investigation is out of equilibrium. First of all we expect that correlations and responses will be generally dependent on the two separate times t and t'. Secondly, explicit violations of FDT will have to show up in equation (7). A parametrization of such violations has been proposed in [18], and consists in generalizing equation (7) to

$$R(t, t') = \beta_{\mathrm{eff}}\frac{\partial C(t, t')}{\partial t'} \tag{10}$$

where $\beta_{\mathrm{eff}} = \beta(C) = \beta X(C)$ is interpreted as an effective temperature. The corresponding integral representation of (10) is

$$\chi(t, t') = \int_{C(t,t')}^{1}\beta(C)\,\mathrm{d}C = \beta\int_{C(t,t')}^{1}X(C)\,\mathrm{d}C. \tag{11}$$

For equilibrium dynamics, $X(C) = 1$ and equation (9) is recovered, while violations will appear for off-equilibrium behaviour, manifesting themselves as deviations from the straight line with slope -1 of the corresponding equilibrium regime.

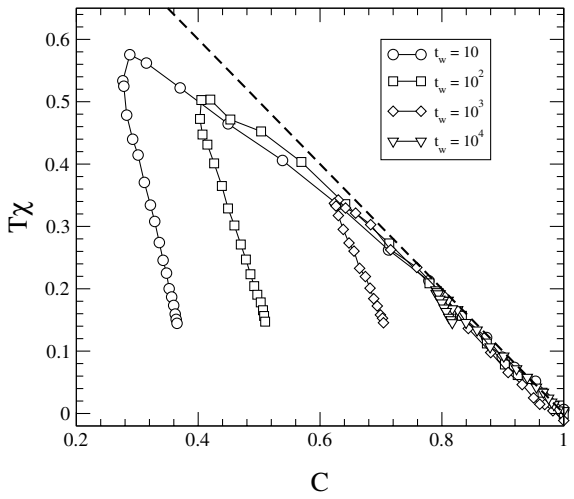

Figure 4. FDT plots in the SCIC for $N = 10^5$, $T = 0.3$ and different waiting times $t_w = 10, 100, 1000, 10\,000$. The straight line is the FDT relation.

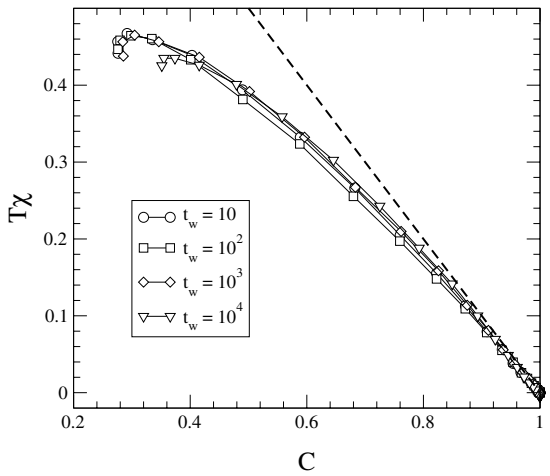

Figure 5. FDT plots in the SCIC for $N = 10^5$, $T = 0.11$ and different waiting times $t_w = 10, 100, 1000, 10\,000$. The straight line is the FDT relation.

We show in figures 4 and 5 two plots of the integrated response function $T\chi = TM_{\text{stag}}/2h_0$ as a function of the correlation for the SCIC model and for two different temperatures. The existence of different activated relaxation times results in rather peculiar FDT plots. For $t_w < \tau_1$ (figure 5) C, χ and X do not show any dependence on t_w; nevertheless X is a non-trivial function of C corresponding to non-equilibrium behaviour without aging. For $t_w > \tau_1$, figure 4, there are aging effects and X shows the typical two-slope pattern. However, the existence of a second typical timescale results in a second downwards bending of the integrated response function and X as function of C has a three-slope shape.

We repeat the same analysis for the ACIC model. In figures 6 and 7 we show the FDT plots for the ACIC at temperatures $T = 0.4$ and 0.2 respectively. Interestingly, for waiting times comparable with the correlation time, such that the system is not too far from equilibrium,

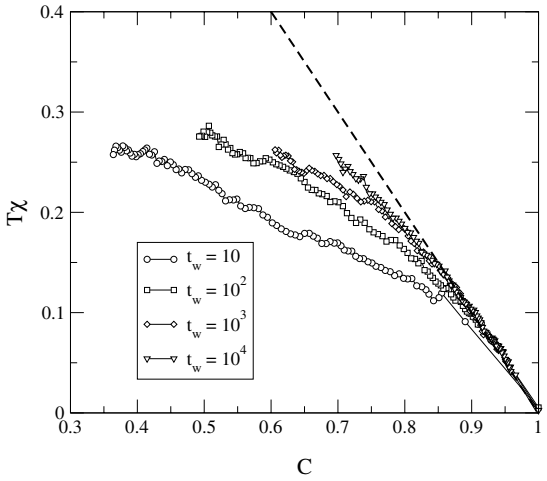

Figure 6. FDT plots in the ACIC for $N = 10^5$, $T = 0.4$ and different waiting times $t_w = 10, 100, 1000, 10\,000$. The straight line is the FDT relation.

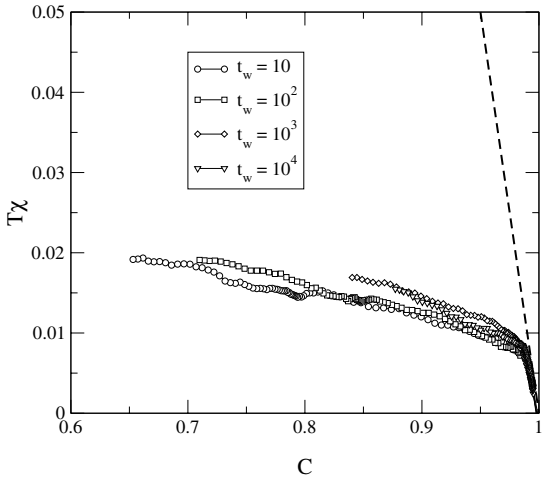

Figure 7. FDT plots in the ACIC for $N = 10^5$, $T = 0.2$ and different waiting times $t_w = 10, 100, 1000, 10\,000$. The straight line is the FDT relation.

the fluctuation-dissipation ratio X rapidly converges to 1; see figure 6. At low temperatures (figure 7), $t_w \ll \tau_{\rm corr}$ and the fluctuation-dissipation ratio is very small, $X \simeq 0.1$, and roughly independent of t_w, a scenario typical of coarsening models [19].

Finally we address the BG model. Our results are shown in figures 8 and 9. Note that aging effects are absent for $t_w < \tau_1$, but nevertheless $X < 1$. For waiting times $\tau_1 < t_w < \tau_{\rm eq}$ the system shows strong non-equilibrium effects with a downwards bending of the integrated response function as a function C, similar to what is seen in the SCIC model. The origin of this effect is, however, different and follows from the asymmetric response of occupied and empty boxes to the staggered field. Since the field is coupled to empty boxes, the typical time to empty a box is larger than that to occupy an empty one. In other words, when quenching from high (or infinite) temperature, boxes are occupied fast and their number converges relatively

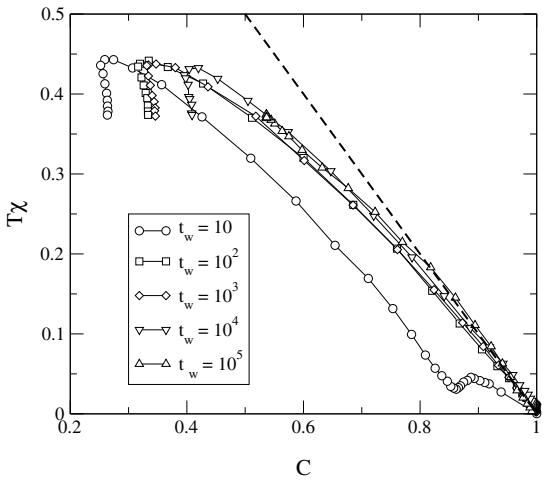

Figure 8. FDT plots in the BG for $N = 10^4$, $T = 0.1$ and different values of t_w.

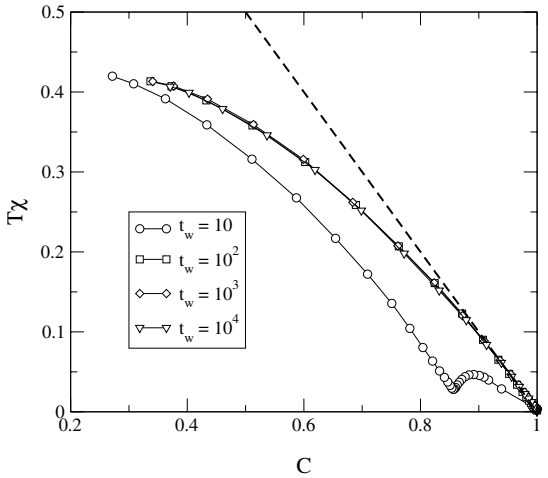

Figure 9. As figure 8, but for $T = 0.09$.

fast towards the equilibrium value. However, due to the staggered field, the distances between them are far from the equilibrium value and occupied boxes must be rearranged, which is a very slow process.

4. The Stillinger and Weber decomposition

An interesting approach to the investigation of activated behaviour in glasses was suggested in the 1980s by SW [7]. As shown in figure 10, each configuration of the system is mapped into a local minimum of the energy through a local potential energy minimization (*quench*) starting from the given configuration. The local minimum was called the IS, while the set of configurations flowing into it defines the *basin of attraction* or *valley* of the IS.

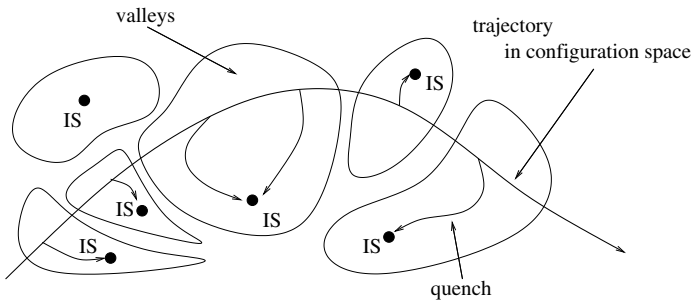

Figure 10. A pictorial description of the SW decomposition. Equilibrium configurations are regularly quenched to reach the corresponding minimum of the phase-space IS. The set of configurations reaching the given minimum is called the basin of attraction or valley of that minimum.

Following SW one constructs an IS-based thermodynamics decomposing the partition function into a sum over IS with the same energy [7]:

$$\mathcal{Z}(T) \simeq \sum_{e} \mathcal{Z}_{\mathrm{IS}}(e, T) \tag{12}$$

with

$$\mathcal{Z}_{\mathrm{IS}}(e, T) = \exp[N(-\beta e + s_{\mathrm{c}}(e) - \beta f(\beta, e))]. \tag{13}$$

Here $s_{\mathrm{c}}(e)$ is the configurational entropy, which yields the number of different IS with energy e:

$$\Omega(e) = \exp(N s_{\mathrm{c}}(e)). \tag{14}$$

The term $f(\beta, e)$ accounts for the free energy of the IS basin of energy e, i.e., the partition sum restricted to the basin of attraction of IS with energy e. In each IS basin the energy has been shifted, so the IS has zero energy, and f accounts only for energy differences. Then the probability of finding an IS with energy e is given by the expression

$$\mathcal{P}_{\mathrm{IS}}(e, T) = \exp[N(-\beta e + s_{\mathrm{c}}(e) - \beta f(\beta, e))]/\mathcal{Z}(T). \tag{15}$$

In general, $f(\beta, e)$ may have a non-trivial dependence on the energy if the IS basin of IS with different energy are different. Usually it is reasonable to expect that $f(\beta, e)$ is roughly independent of e at least in two different situations. The first is when the temperature is such that only the states near the bottom of the IS basin contribute [8, 9], and the second is when the IS basins are narrow and contain few configurations, as in REM-like models [9, 20].

When the e-dependence of f can be neglected, the configurational entropy $s_{\mathrm{c}}(e)$ can be obtained directly from (13). From an operative point of view, the procedure that we followed consists in the following steps:

(i) We equilibrate the system at temperature T with t_{therm} Monte Carlo steps (MCS).
(ii) We run a group of t_{run} MCS. At the end of the group we perform a steepest-descent procedure ($T = 0$ Monte Carlo dynamics) to identify an IS.
(iii) We repeat step 2 N_{run} times.
(iv) We keep in memory the number of times N_{IS} that we have found an IS with a given energy e.
(v) We construct the histogram $\mathcal{P}_{\mathrm{IS}}(e, T)$.
(vi) We calculate $s_{\mathrm{c}}(f, T)$ as

$$s_{\mathrm{c}}(e) = \beta e + \frac{1}{N} \log \mathcal{P}_{\mathrm{IS}}(e, T) + \Delta(T) \tag{16}$$

where

$$\Delta(T) = \beta f(\beta) + \frac{1}{N} \log \mathcal{Z}(T) \tag{17}$$

is assumed to be a function of temperature only, and is computed by imposing the collapse of the data points onto a single curve.

The replacement of the original partition function (12) with the sum of the partition functions in each valley is expected to be valid and to reproduce the correct thermodynamics since it corresponds simply to a different way of summing the partition function. Of course this is true within the approximation that all the valleys have the same relevance to the statistical properties of the system. The scenario that we are proposing rests on the idea that to describe the equilibrium properties of the system it is sufficient to count its IS. In other words we implicitly assume the existence of an equiprobability principle working for the IS themselves, according to which the frequency of visits to an IS with a given energy is only dependent on the total number of IS present in the system at that energy. Then the configurational entropy can be considered as analogous to the ordinary Boltzmann entropy, which in the Gibbs ensemble counts the number of configurations with a given energy. In contrast, if the frequency of visits to a given IS is also dependent on different parameters, then such a construction may not work. An example of this is the Sherrington–Kirkpatrick model, where the size of the basins must also be taken into account. In this case, for the configurational entropy to be meaningful it needs to be expressed in terms of the free energy of the valleys, not in terms of their potential energies [10].

However, the definition of the SW projection is also dynamical by its own nature, and contains relevant information about the off-equilibrium properties of the system. This is due to the intrinsically dynamical way of defining the IS themselves, which is through a quenching procedure based on the dynamics of the system. This partially answers the criticism recently raised by Biroli and Monasson [21] about the definition of the IS itself. On the other hand, that criticism remains meaningful in that it highlights how the configurational entropy, even though well defined, may not be able to capture the relevant dynamics of the system. According to its definition, the configurational entropy not only contains information about the equilibrium properties of the system, but also on how the system approaches equilibrium. As we shall see, this is the key point that makes the SW decomposition unsuitable for coarsening systems such as the ones discussed in this paper.

We have calculated the configurational entropy analytically for all the models presented. For both the SCIC and the ACIC it is possible to show [6] that the zero-temperature dynamics can be solved exactly and that $\mathcal{P}_{\rm IS}(e, T)$ has the form

$$\mathcal{P}_{\rm IS}(e, T) = \frac{1}{\sqrt{2\pi \langle C_0^2(\infty)\rangle_{\rm c}}} \exp\left(-\frac{(e - \langle e_{\rm IS}\rangle)^2}{2\langle C_0^2(\infty)\rangle_{\rm c}} \right) \tag{18}$$

where $\langle e_{\rm IS}\rangle$ and $\langle C_0^2(\infty)\rangle_{\rm c}$ are known in terms of the equilibrium magnetization (see [6]). Also counting the number of fixed points of the dynamics can produce an estimate of the configurational entropy, which results in [6]

$$s_{\rm c}(e) = \frac{\log(N_{\rm fix})}{N} = -e \log(-e) - (1 + e) \log(1 + e) + (1 + 2e) \log(-1 - 2e). \tag{19}$$

The main point to highlight here is that both these results, equation(18) and (19), are the same for the SCIC as for the ACIC model. As a consequence, we expect the two models to have the same configurational entropy.

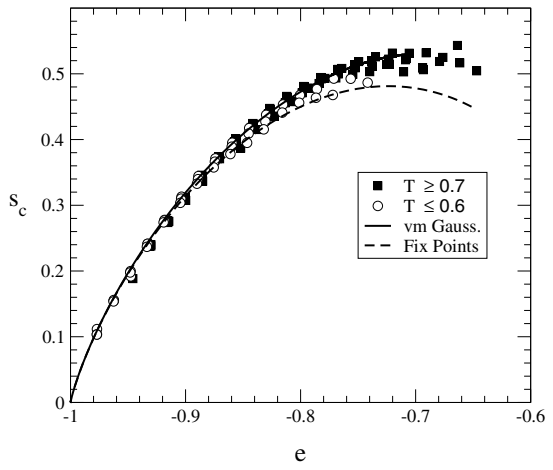

Figure 11. SW configurational entropy in the SCIC for $N = 64$ spins at different temperatures compared with the analytical prediction (22) (upper curve) and the fixed-point estimate (19) (lower curve).

In the case of the BG model, the zero-temperature dynamics cannot be closed exactly. However, we can still carry out an estimation of the configurational entropy by counting the number of fixed points. In this case we obtain [6]

$$s_c(e) = -(1+e)\log(1+e) - e\log(-e) + (1+2e)\log(-1-2e) - \log(y) + (1+e)\log(\exp(y) - y - 1) \tag{20}$$

where y satisfies the saddle-point condition

$$e = -1 + \frac{\exp(y) - 1 - y}{y(\exp(y) - 1)}. \tag{21}$$

Note that for the BG model the configurational entropy may be negative because particles are distinguishable.

We show both the analytical predictions and the numerical data in figures 11 and 12. In figure 11 we show the results obtained for the SCIC model with $N = 64$ and different temperatures. The SW configurational entropy s_c is obtained from the numerical $\mathcal{P}_{IS}(T, e)$ as in equation (16). For each temperature, $\Delta(T)$ has been fixed by collapsing different data onto a single curve. For comparison, we also show the theoretical predictions from equations (19) and (see [6]):

$$s_c(e) = \int_0^T \frac{d\langle e_{IS}\rangle}{dT}\frac{dT}{T}. \tag{22}$$

As shown in [6], they coincide, asymptotically, close to the ground-state energy $e = -1$. The collapse is excellent, showing that the approximation (19) and the low-temperature behaviour (22) asymptotically coincide in the limit $T \to 0$. We note that there is a range of energies where data from $T \leqslant 0.6$ collapse onto one curve while data for higher temperature collapse onto a different curve. This residual temperature dependence follows from the presence of many equivalent directions for energy minimization [6]. We have checked that $\mathcal{P}_{IS}(e, T)$ is the same for the ACIC model. In all cases we find the same results.

In figure 12 we show the numerical computation of s_c for the BG model, for two different sizes $N = 100, 500$ and temperatures ranging from $T = 0.1$ up to 1. Similarly to what we

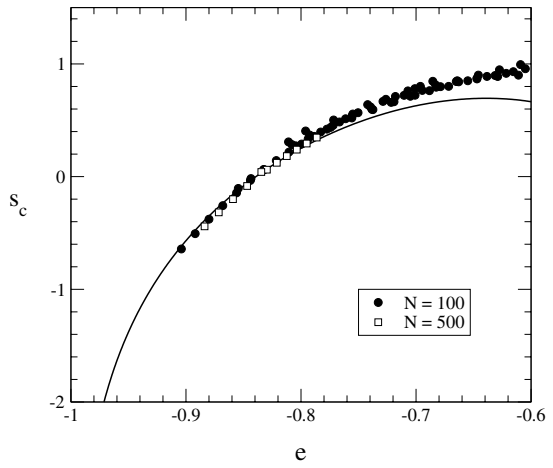

Figure 12. SW configurational entropy in the BG model for $N = 100, 500$ boxes at different temperatures $T = 1.0, 0.5, 0.4, 0.3, 0.2, 0.15, 0.1$ compared with the fixed-point estimate (20) (full line).

found for the constrained kinetic models, the data collapse nicely onto a single curve although they do not exactly coincide with prediction derived from the number of fixed points. In this model the presence of different equivalent directions for decreasing the energy does not influence s_c. This is most probably due to the global character of the constraint.

Comparing figures 11 and 12 we see that the agreement between measured and predicted configurational entropy is now worse. We attribute this to the presence of entropic barriers which follows from all possible arrangements of particles inside the boxes. All arrangements leave the energy unchanged, but their number strongly depends on the number of empty boxes, leading to a stronger energy dependence of the IS free energy for this model. This effect is not present in the kinetically constrained Ising chain.

The conclusion that can be drawn from this section is that for the models considered a description of their glassy behaviour in terms of a complex energy landscape is not relevant. Even though the SW configurational entropy for the constrained Ising chain is a non-trivial quantity, it does not distinguish the SCIC model from the ACIC model.

5. Concluding remarks

In this paper we have analysed the possibility of decomposing the dynamics of 1D constrained models according to the SW prescription [7].

In particular we have focused on the SCIC and ACIC [2,3] and on the BG model [16]. All these models have been proven to exhibit glassy and coarsening behaviour. Their approaches to equilibrium have turned out to be quite different, due to the different microscopic kinetic constraints. This was apparent specifically in their different fluctuation-dissipation plots.

In contrast the SW projection always results in configurational entropies with the same qualitative features. We argue that this is related to the fact that a growing length scale is present in these systems, driving the equilibration processes. In other words, when one replaces the original dynamics with an IS-based dynamics, one is not able to transfer to the IS level the information about the correlation between the successive configurations reached during the approach to equilibrium. If the system under consideration evolved between

uncorrelated configurations, then the SW approach would be powerful, as has been proved in other cases [9, 10]. However, here the missing coarsening-biased choice in the jumps between an IS and the following one prevents it from working properly.

The SW approach is expected to hold for systems where the relevant equilibration is driven by an entropic process, with activated jumps between different basins occurring with the same probability [22].

Discerning a good class of simple and tractable models which contain the relevant mechanisms responsible for relaxation in real glasses would be a very important step in the direction of building a microscopic theory for the glass transition beyond ideal mode-coupling theory.

References

[1] Rubí M and Perez-Vicente C (ed) 1996 Complex behaviour in glassy systems *Proc. 14th Sitges Conf. 1995* (Berlin: Springer)
Angell C A 1995 *Science* **267** 1924
[2] Fredrickson G H and Andersen H C 1984 *Phys. Rev. Lett.* **53** 1244
[3] Jäckle J and Eisinger S Z 1991 *J. Phys.: Condens. Matter* **84** 115
[4] Sollich P and Evans M R 1999 *Phys. Rev. Lett.* **83** 3238
[5] Majumdar S N, Dean D S and Grassberger P 2001 *Phys. Rev. Lett.* **86** 2301
[6] Crisanti A, Ritort F, Rocco A and Sellitto M 2000 *J. Chem. Phys.* **113** 10 615
[7] Stillinger F H and Weber T A 1982 *Phys. Rev.* A **25** 978
[8] Sciortino F, Kob W and Tartaglia P 1999 *Phys. Rev. Lett.* **83** 3214
Kob W, Sciortino F and Tartaglia P 2000 *Europhys. Lett.* **49** 590
[9] Crisanti A and Ritort F 2000 *Europhys. Lett.* **51** 147
Crisanti A and Ritort F 2000 *Europhys. Lett.* **52** 640
[10] Crisanti A, Marinari E, Ritort F and Rocco A 2001 *Preprint* cond-mat/0105391
[11] Note that the definition here adopted for d is different from the one adopted in [4]. In our case, we do not consider the border of the domains in the computation of their size. The two definitions differ by one unit.
[12] Follana E and Ritort F 1996 *Phys. Rev.* B **54** 930
[13] Reiter J and Jackle J 1995 *Physica* A **215** 311
[14] Schulz M and Trimper S 1999 *J. Stat. Phys.* **94** 173
[15] Mauch F and Jackle J 1999 *Physica* A **262** 98
[16] Ritort F 1995 *Phys. Rev. Lett.* **75** 1190
[17] Godreche C, Bouchaud J P and Mezard M 1995 *J. Phys. A: Math. Gen.* **28** L603
Franz S and Ritort F 1996 *J. Stat. Phys.* **85** 131
[18] Cugliandolo L F and Kurchan J 1993 *Phys. Rev. Lett.* **71** 173
[19] Barrat A 1998 *Phys. Rev.* E **57** 3629
[20] Derrida B 1981 *Phys. Rev.* B **24** 2613
[21] Biroli G and Monasson R 2000 *Europhys. Lett.* **50** 155
[22] Crisanti A and Ritort F 2001 *Preprint* cond-mat/0102104